Langmuir

ARTICLE

pubs.acs.org/Langmuir

One-Pot Tuning of Au Nucleation and Growth: From Nanoclusters to Nanoparticles

Sheng-Feng Lai,[†,‡] Wen-Chang Chen,[‡] Cheng-Liang Wang,[†] Hsiang-Hsin Chen,[†] Shin-Tai Chen,[†] Chia-Chi Chien,[†,§] Yi-Yun Chen,[†] Wen-Ting Hung,[†] Xiaoqing Cai,[†] Enrong Li,[†] Ivan M. Kempson,[†] Y. Hwu,[*,†,§,∥] C. S. Yang,[⊥] Eng-Soon Tok,[#] Hui Ru Tan,[▽] Ming Lin,[▽] and G. Margaritondo[○]

[†]Institute of Physics, Academia Sinica, Nankang, Taipei 11529, Taiwan

[‡]Department of Chemical and Materials Engineering, National Yunlin University of Science and Technology, Douliou, Yunlin 64002, Taiwan

[§]Department of Engineering and System Science, National Tsing Hua University, Hsinchu, Taiwan

[∥]Institute of Optoelectronic Sciences, National Taiwan Ocean University, Keelung 20224, Taiwan

[⊥]Center for Nanomedicine, National Health Research Institutes, Miaoli 35053, Taiwan

[#]Physics Department, National University of Singapore, Singapore 117542

[▽]Institute of Materials Research and Engineering, 3 Research Link, Singapore 117602

[○]Ecole Polytechnique Fédérale de Lausanne (EPFL), CH-1015 Lausanne, Switzerland

Supporting Information

ABSTRACT: We describe a simple and effective method to obtain colloidal surface-functionalized Au nanoparticles. The method is primarily based on irradiation of a gold solution with high-flux X-rays from a synchrotron source in the presence of 11-mercaptoundecanoic acid (MUA). Extensive tests of the products demonstrated high colloidal density as well as excellent stability, shelf life, and biocompatibility. Specific tests with X-ray diffraction, UV−visible spectrometry, visible microscopy, Fourier transform infrared spectroscopy, dark-field visible-light scattering microscopy, and transmission electron microscopy demonstrated that MUA, being an effective surfactant, not only allows tunable size control of the nanoparticles, but also facilitates functionalization. The nanoparticle sizes were 6.45 ± 1.58, 1.83 ± 1.21, 1.52 ± 0.37 and 1.18 ± 0.26 nm with no MUA and with MUA-to-Au ratios of 1:2, 1:1, and 3:1. The MUA additionally enabled functionalization with L-glycine. We thus demonstrated flexibility in controlling the nanoparticle size over a large range with narrow size distribution.

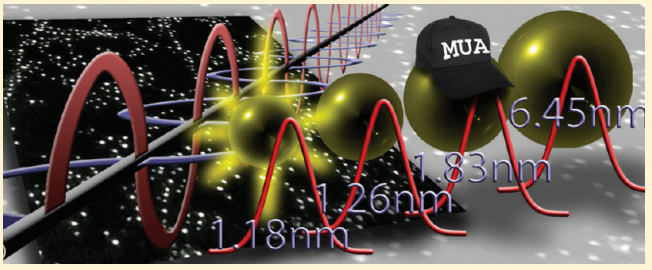

Gold nanoscaled structures have very high scientific and technological interest in diverse fields.[1] In biomedical applications, the role of nanoparticles (NPs) does not merely depend on chemistry, composition, or their functionalization. There are fundamental size effects that alter cellular interactions and influence response and expression.[2] The importance of size-control and size confinement is increasingly taken into consideration for the possible biomedical use of NPs. Significant changes in cytotoxicity were observed even for small changes in NP size,[3] therefore effective control is required for optimizing the desired effects. The general conclusion is that accurate size control is an important prerequisite for the full exploitation of Au NP properties.[5−11]

Here we demonstrate a one-pot Au NP synthesis approach utilizing intense X-ray irradiation in the presence of 11-mercaptoundecanoic acid (MUA) to produce NPs with sizes from tens of atoms up to much larger values. This approach offers control over parameters such as the evolution time and rate of nucleation, which can be manipulated to tailor the Au NP size while maintaining a small size distribution. Additionally, the diameters surpass the Au cluster sizes reported for other methods, for example, 1.4 nm for Au55 clusters.[4] Near spontaneous, homogeneous reaction induction occurs with high reaction rates and ensures uniformity within the reaction vessel.

Highly functional Au NPs have been synthesized by several means, often utilizing a templating approach or via chemical reduction within a different solution.[12−21] These approaches, however, imply the added complexity of template removal or have inherent limitations due to reaction rate kinetics. Particularly interesting work by Shields et al. demonstrated the necessity in acquiring control over the nucleation, specifically to control the nucleation rate and the nucleation time window (Δt) to optimize the NP mean sizes and their size distributions.[22]

Bogush and Zukoski demonstrated that nucleated clusters aggregate in time scales faster than typical growth processes.[23]

Received: March 8, 2011
Revised: April 1, 2011
Published: June 01, 2011

Downloaded via ECOLE POLYTECHNIC FED LAUSANNE on July 11, 2020 at 13:17:17 (UTC).
See https://pubs.acs.org/sharingguidelines for options on how to legitimately share published articles.

 © 2011 American Chemical Society dx.doi.org/10.1021/la200861e | *Langmuir* 2011, 27, 8424–8429

Agglomerated particles are typically undesirable because of their nonuniform shapes and sizes.[24,25] Our approach however, completes synthesis in subsecond time and can reduce the aggregative growth of particles. The presence of a controlled number of nuclei confirms the ability to control the NP size.[26] Additionally, we hypothesize that significant electrostatic stabilization facilitates the achievement of monodispersive character (due to the ionizing radiation) and reduces aggregation of nanocrystallites. This can prevent the formation of larger particulates by a classical LaMer-like approach, with separate nucleation and growth phases.

Our technique reaches size control via a single synthesis method rather than using different methods for different size ranges, and has no need for strong reducing agents or thermal acceleration.[3,27,28] The chemically simplified environment (i.e., no reducing agents) enhances biocompatibility, and the absence of purification procedures can facilitate up-scaling the synthesis to large volumes.

A key factor in our technique was the use of very intense X-ray irradiation. This makes the reaction easy to control, specifically triggered and terminated with high precision and very rapidly. X-rays lead to ion reduction by radiolysis of the solvent, in our case water, producing free radicals like H• and free electrons that act as reducing agents. With very intense X-rays, the resulting reduction is very fast, and the NP nucleation starts uniformly. These favorable characteristics allow us to successfully synthesize very small Au NPs, ∼1 nm with narrow size distribution and excellent colloidal stability, without access to physical templates such as dendrimers and micelle. The process therefore not only simplifies the synthesis and increase the control on the reaction, but reduces the possible negative effects of more complicated purification process.

NP synthesis by X-ray irradiation was already used, either without surface coating[29] or in the presence of polyethylene glycol (PEG).[30,31] The new element here is irradiation in the presence of MUA, a more effective surfactant than PEG since the thiol group directly binds to the Au in the growing NPs. This prevents further aggregation immediately after the nucleation. We showed that the resulting MUA-coated Au NP is biocompatible and can be used as a linker to conjugate other molecules, such as L-glycine.

EXPERIMENTAL SECTION

Materials. $HAuCl_4 \cdot 3H_2O$, MUA, dicyclohexylcarbodiimide (DCC), L-glycine, and sodium hydroxide were purchased from Sigma-Aldrich. Dimethyl sulfoxide (DMSO) and *N*-hydroxysuccinimide (NHS) were purchased from J.T. Baker and Alfa Aesar. Dulbecco's modified Eagle medium and F12 (DMEM/F12) and phosphate-buffered saline (PBS) were purchased from Gibco and UniRegion Biotech, respectively. All chemicals were reagent grade. Distilled deionized (d.d.) water was purified with a Millipore Milli-Q water system.

X-ray synthesis. The synthesis followed a one-pot procedure. Solutions were prepared with 0.5 mL of 20 mM $HAuCl_4 \cdot 3H_2O$, adjusted to pH ∼10 with 0.1 M NaOH. MUA was added in 0.2 mL in anhydrous ethanol with molar concentrations (relative to Au) of 1:2, 1:1, and 3:1, and increasing the volume to 10 mL with water. Each solution was diluted to half concentration up to 300 μL with water (to ensure a sufficiently transparent solution for real time UV−visible monitoring) in a cuvette and irradiated with hard X-rays from the BL01A beamline of the National Synchrotron Radiation Research Center (NSRRC), Hsinchu, Taiwan, running at a constant electron current of 300 mA by a top-up injection every minute. The X-ray photon energy ranged from 8 to 15 keV and was centered at ∼12 keV with a dose rate of $\sim 4.7 \times 10^5$ Gy s^{-1}.[32] The irradiation were performed on small volume (0.3 mL), and the X-ray beam illuminated the complete volume. The irradiation time for each synthesis was 1 s, determined by the opening time of an X-ray shutter. Considering the mean photon energy (12 keV) and the average energy required to reduce a Au ion (∼25 eV), $\sim 1.5 \times 10^{19}$ of Au ions can be reduced with less than 1 s of irradiation. With 1.8×10^{17} Au ions present in the initial solution, we can indeed estimate that the reduction is completed within a much shorter time.

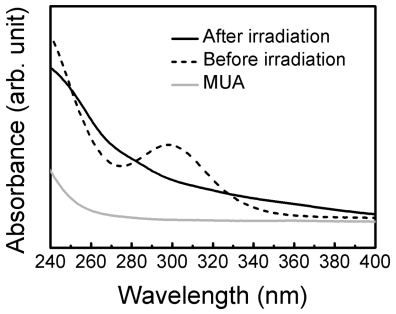

Figure 1. UV−visible spectral analysis of precursors and MUA-coated NPs: A precursor solution with a 3:1 molar MUA:Au ratio before and after irradiation by X-rays for 1 s; and for comparison, a pure 1.5 mM MUA solution.

UV−Visible Absorption. Spectra were acquired over 200−800 nm using a USB4000 Fiber Optic spectrometer from Ocean Optics (Dunedin, USA) with 1 cm path length quartz cuvette (Evergreen Scientific, USA).

Transmission Electron Microscopy (TEM). Sample were prepared by placing a drop of solution on a carbon-coated copper grid and dried at 40 °C. TEM measurements were performed in a JEOL JEM-2100F system with a 4096 × 4096 CCD imaging system (Gatan, UltraScan 4000) operated with an accelerating voltage of 200 kV. At high magnification imaging mode used for this study, the pixel size is as small as ∼0.057 nm. High-angle annular dark-field (HAADF) scanning transmission electron microscopy (STEM) was performed on MUA-AuNPs with size <2 nm.

Cell Viability. 1.5×10^3 EMT-6 murine breast carcinoma cells per well were seeded in a DMEM/F12 (Gibco, Basel, Switzerland) nutrient mixture containing 10% fetal bovine serum (FBS), 1% antibiotics (penicillin at 100 U mL^{-1} and streptomycin at 100 μg mL^{-1}) and L-glutamine, in a 24-well plate at 37 °C in a humidified 5% CO_2 atmosphere. After 24 h, the MUA-coated Au NPs were added and cocultured for 24 h, followed by the addition of 100 μL methylthiazoletetrazolium solution (MTT; Sigma, St Louis, MO; 5 mg mL^{-1}) for another 2 h culture. After incubation, the medium was removed, 100 μL of DMSO was added, and the samples were incubated at 37 °C for 30 min with constant shaking. Optical absorbance was measured at 570 nm using a microplate reader (Elx 800, Biotek), and the cell viability so evaluated was expressed as percent relative to untreated control cells ($n = 3$).

RESULTS AND DISCUSSION

The numerical estimates presented above of the rapidity of the reaction were confirmed by the experimental results. The spectra of Figure 1 show for example that the reaction was completed before 1 s. Indeed, gold ions produce a distinctive peak at ∼300 nm, which disappeared after 1 s of irradiation of the solution.

In addition to facilitating the surface functionalization, a second likely effect of MUA is to reduce the time frame over which growth occurs, by binding to the Au on the NP surface and capping it. As an active ingredient to terminate the nucleation

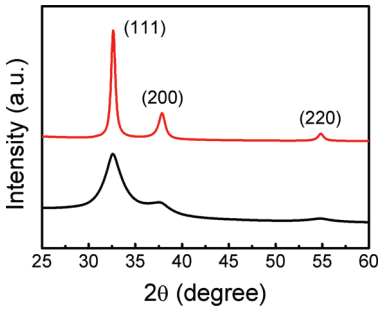

Figure 2. XRD patterns of Au NP colloidal solutions obtained with and without MUA. The black curve was produced after irradiation of a precursor solution with a 1:1 molar ratio of MUA to $HAuCl_4 \cdot 3H_2O$. The red curve was obtained with no MUA. The three peaks correspond to the (111), (200), and (220) planes of metallic gold and are visibly narrower when MUA was absent from the precursor solution. This indicates the formation of larger particles than those obtained in the presence of MUA.

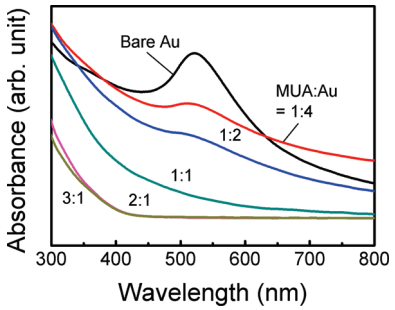

Figure 3. UV−visible spectra of colloidal Au NPs obtained by varying the relative MUA: Au molar concentrations.

and growth of Au NP, MUA is particular advantageous for its high affinity with Au. Even with the lowest concentration of MUA, reactions are completed on a subsecond time scale. For high MUA concentrations, we can expect nucleation times $\Delta t \ll 1$ s. The X-ray source used here delivers a dose of 2−5 orders of magnitude larger than previously reported.[33,34] The lower photon energies, in the kiloelectron volt range as opposed to the megaeelectron volt produced by γ-sources, allow stronger interaction with the solvents and Au precursors and NPs. Finally, we note that the high synthesis efficiency made possible by intense X-rays is important for scaled-up production as required by many possible applications.

The suspension produced by irradiation exhibits a high degree of stability that can be attributed to the MUA (Figure S1 in the Supporting Information). Without MUA, the UV−visible spectrum continues to evolve with time, suggesting further Ostwald and/or aggregative growth. The excellent dispersion of the MUA-capped particles was confirmed with dark-field visible-light scattering microscopy and UV−visible spectroscopy in DMEM/F12, 1X PBS, and d.d. water (Figure S2 in the Supporting Information). No aggregation was indeed observed in these tests.

The fact that the presence of MUA leads to small-size particles was corroborated by X-ray diffraction (XRD) analysis. The black curve was produced after irradiation of a precursor solution with a 1:1 molar ratio of MUA to $HAuCl_4 \cdot 3H_2O$. The red curve was obtained with no MUA present. XRD peaks in Figure 2 corresponding to (111), (200), and (220) planes of metallic gold are clearly narrower in the absence of MUA. This reveals the formation of larger particles than those obtained in the presence of MUA.

Effects of the MUA concentration in the precursor solution are revealed by the UV−visible spectra of Figure 3. The surface plasmon peak varies based on precursor concentrations. It is clear that the peak intensity is reduced and finally eliminated as the MUA concentration increases. This indicates that the MUA progressively decreases the NP size until the plasmon peak disappears. The spectral shift of the peak (from ∼493 to ∼522 nm) supports the same conclusion. Note that when the MUA-to-$HAuCl_4 \cdot 3H_2O$ ratio increases from 1:1 to 3:1, the peak disappears, indicating an average particle size of <2 nm.[35] The most direct evidence of the effects of MUA on the synthesis is provided by the results of high-resolution field emission gun TEM (FEG-TEM) like those shown in Figure 4. However, the low contrast of very small particles could result in an underestimate of the particle size. Dark-field STEM (HAADF-TEM in Figure 5) was therefore used to provide more accurate size measurement for the 1:1 ratio and 3:1 ratio specimens. These tests yielded sizes significantly larger than bright-field TEM: 1.2 nm versus 1.5 nm for the 1:1 specimen and 0.8 nm versus 1.2 nm for the 3:1 specimen; this confirms the negative impact of low contrast. However, dark-field imaging confirmed that the particle size of both specimens was <2 nm with good size uniformity, and that a higher MUA concentration reduces the size.

The ability to increase the particle functionalization was confirmed by subjecting the nanosols to sequential concentration steps with centrifugation and redilution to remove unbound MUA, followed by conjugation with L-glycine and Fourier transform infrared (FTIR) analysis (Figure S3 in the Supporting Information). Absorbance bands due to amide bond formation were observed at 1624 and 1536 cm^{-1} corresponding to the C═O stretching band (Amide I) and to the −NH bending vibration band (Amide II) and the peak at 3322 cm^{-1} due to the N−H band between amides.[36,37]

Finally, preliminary cell viability tests demonstrated that the MUA-coated gold NPs obtained here have good biocompatibility. The results are similar to those previously obtained, for example, with PEG-coated gold NPs also produced by X-ray irradiation.[38,39]

Cell viability for all MUA:Au ratios demonstrates high biocompatibility (Figure 6). Only when the Au concentration reached 1 mM did the viability decrease to near 80%. We did not observe variations as a function of the particle size. However, we cannot exclude the occurrence of other effects on the cellular expression.

We previously found that with attenuated X-ray intensity, the reaction rates can be slowed down.[40] Therefore, the nucleation rate can be also controlled with our synthesis approach. Further experiments are underway to test the feasibility of control and characterization in the milli- to microsecond range, to produce even smaller gold atomic clusters and NPs with narrow distributions.

The combination of analytical characterization provides good evidence that MUA can be used in combination with X-ray irradiation to control the size of colloidal Au NPs. Specifically, MUA in the precursor solution (1) prevents aggregation of NPs, (2) results in smaller NPs, and (3) results in a narrower size distribution. Such conclusions were coherently supported by all of the tests performed. They additionally provided evidence for the phenomena underlying these findings. Basically, the synthesis is sufficiently fast and capped by MUA to prevent aggregative or Ostwald growth.

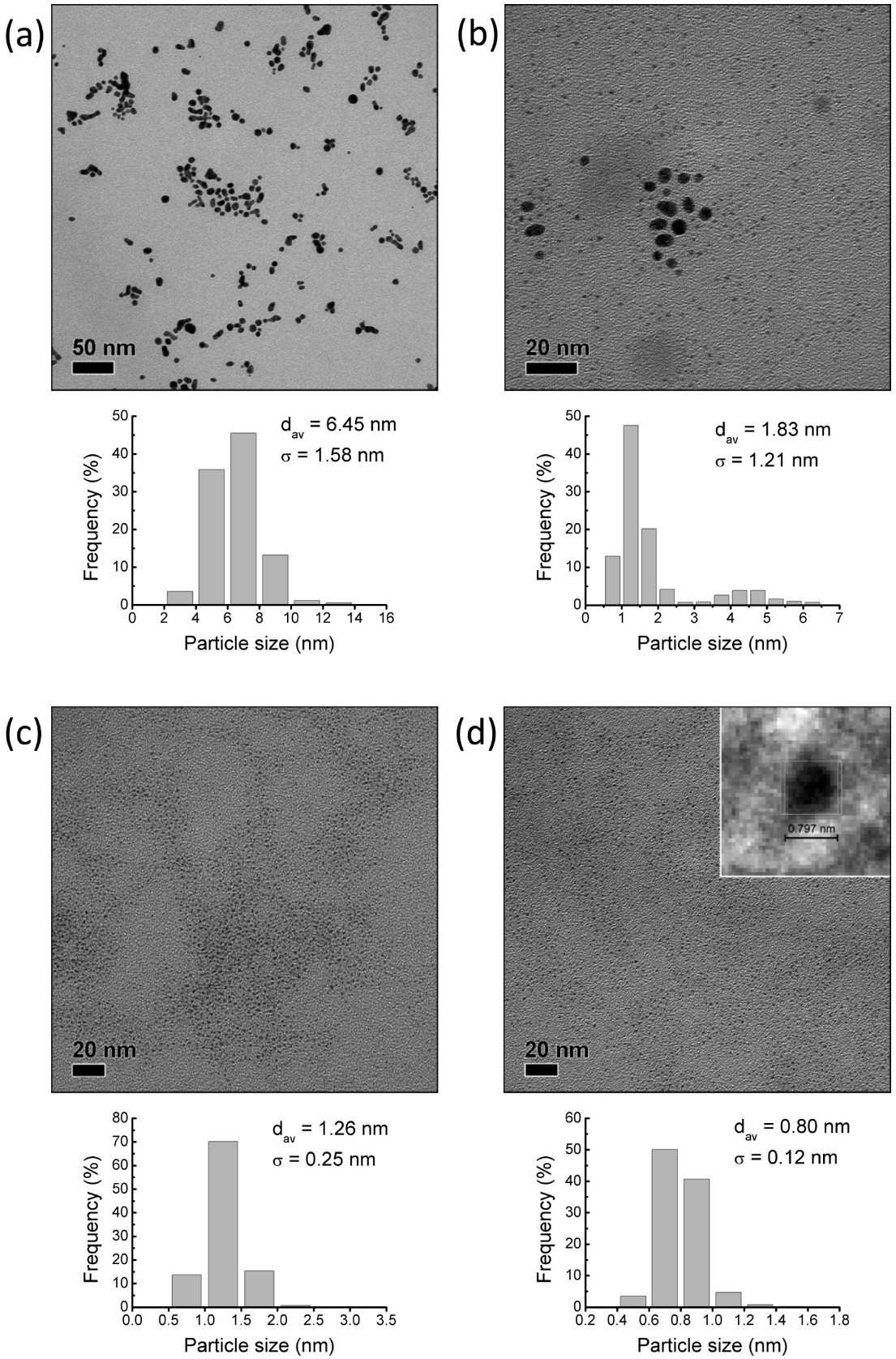

Figure 4. TEM micrographs of Au NPs synthesized in the absence of MUA and increasing MUA concentrations and corresponding size histograms ($n > 500$). Large, nonspherical NPs result with no MUA present (a). With an increasing ratio of MUA:Au of 1:2 (b), 1:1 (c), and 3:1 (d), the resulting NP dimensions and standard deviation decrease. Inset: A magnified TEM image for a small Au NP.

dx.doi.org/10.1021/la200861e |*Langmuir* 2011, 27, 8424–8429

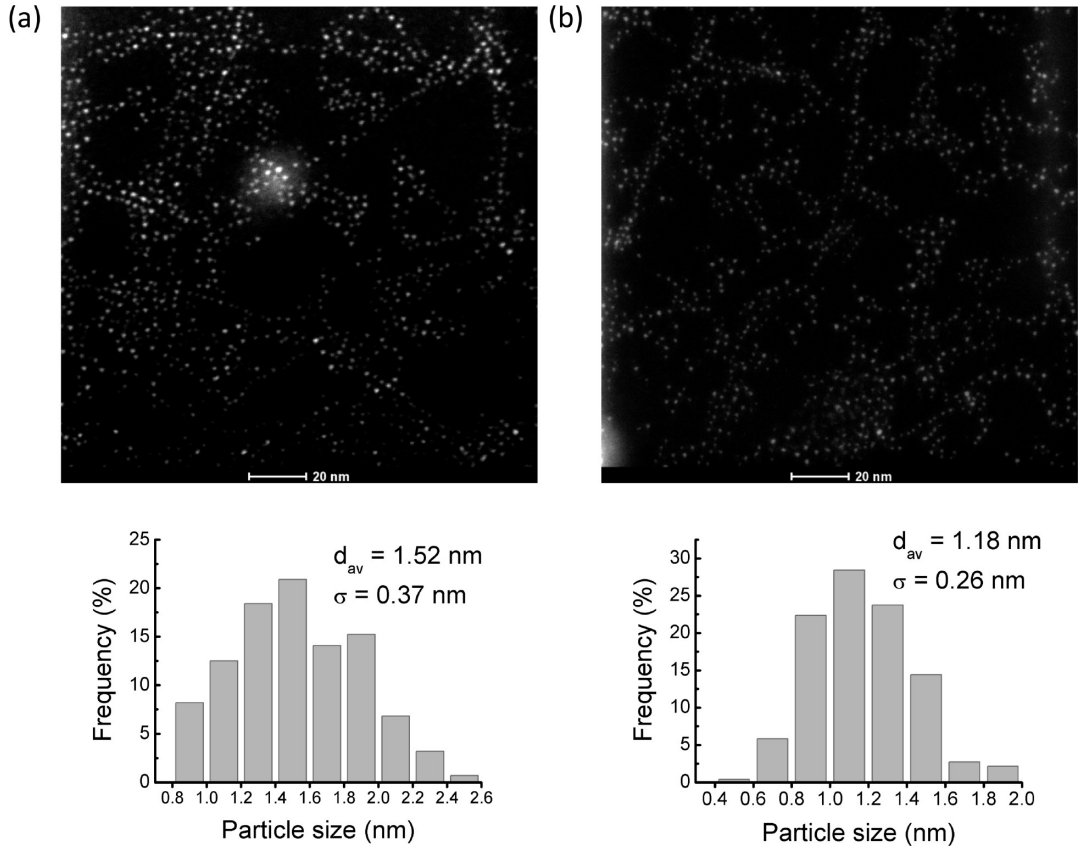

Figure 5. Dark-field STEM micrographs of Au NPs synthesized in the absence of MUA and increasing MUA concentrations and corresponding size histograms (n > 500). With a ratio of MUA:Au of 1:1 (a) and 3:1 (b), the resulting NP dimensions and standard deviation decrease.

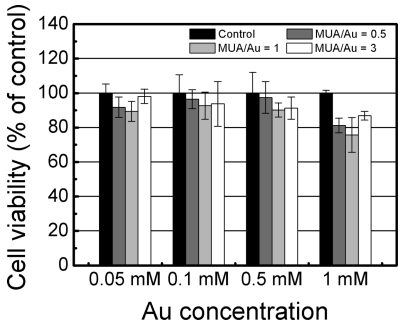

Figure 6. Cell viability of EMT-6 cells cocultured with different molar ratios of MUA:Au at different Au concentrations for 24 h.

This approach could be extended to other colloidal NP systems and to different surfactants. Therefore, it could provide a general class of solutions for the critical issue of controlling colloidal NP sizes, with a broad range of potential applications.

■ ASSOCIATED CONTENT

Supporting Information. UV-visible spectra of colloidal gold NP solutions synthesised with and without MUA; UV–visible spectra and colloidal stability test of AuNPs-MUA by dark field microscopy in d.d. water, 1X PBS, and DMEM/F12 medium; FTIR spectra of MUA and MUA-coated Au NPs before and after L-glycine conjugation; and experimental details. This information is available free of charge via the Internet at http://pubs.acs.org/.

■ AUTHOR INFORMATION

Corresponding Author

*E-mail: phhwu@sinica.edu.tw, chenwc@yuntech.edu.tw.

■ ACKNOWLEDGMENT

This research was supported by the National Program for Nanoscience and Nanotechnology, the Thematic Research Project of Academia Sinica, the Biomedical Nano-Imaging Core Facility at the National Synchrotron Radiation Research Center (Taiwan), the Fonds National Suisse pour la Recherche Scientifique, and by the Center for Biomedical Imaging (CIBM, supported by the Louis-Jeantet and Leenards foundations).

■ REFERENCES

(1) Giljohann, D. A.; Seferos, D. S.; Daniel, W. L.; Massich, M. D.; Patel, P. C.; Mirkin, C. A. Gold nanoparticles for biology and medicine. *Angew. Chem., Int. Ed.* **2010**, *49*, 3280–3294.

(2) Jiang, W.; Kim, B. Y. S.; Rutka, J. T.; Chan, W. C. W. Nanoparticle-mediated cellular response is size-dependent. *Nat. Nanotechnol.* **2008**, *3*, 145–150.

(3) Pan, Y.; Neuss, S.; Leifert, A.; Fischler, M.; Wen, F.; Simon, U.; Schmid, G.; Brandau, W.; Jahnen-Dechent, W. Size-dependent cytotoxicity of gold nanoparticles. *Small* **2007**, *3*, 1941–1949.

(4) Schmid, G.; Pfeil, R.; Boses, R.; Bandermann, F.; Meyer, S.; Calis, G. H. M.; van der Velden, J. W. A. $Au_{55}[P(C_6H_5)_3]_{12}CI_6$ - Ein goldcluster ungewöhnlicher grösse. *Chem. Ber.* **1981**, *114*, 3634–3642.

(5) Cao, Y. C.; Jin, R. C.; Nam, J. M.; Thaxton, C. S.; Mirkin, C. A. Raman dye-labeled nanoparticle probes for proteins. *J. Am. Chem. Soc.* **2003**, *125* (48), 14676–14677.

(6) Hainfeld, J. F.; Slatkin, D. N.; Focella, T. M.; Smilowitz, H. M. Gold nanoparticles: A new X-ray contrast agent. *Brit. J. Radiol.* **2006**, *79* (939), 248–253.

(7) Jain, P. K.; Lee, K. S.; El-Sayed, I. H.; El-Sayed, M. A. Calculated absorption and scattering properties of gold nanoparticles of different size, shape, and composition: Applications in biological imaging and biomedicine. *J. Phys. Chem. B* **2006**, *110* (14), 7238–7248.

(8) Jana, N. R. Gram-scale synthesis of soluble, near-monodisperse gold nanorods and other anisotropic nanoparticles. *Small* **2005**, *1* (8−9), 875–882.

(9) Wang, L. H.; Li, J.; Song, S. P.; Li, D.; Fan, C. H. Biomolecular sensing via coupling DNA-based recognition with gold nanoparticles. *J. Phys. D: Appl. Phys.* **2009**, *42* (20), 203001–203011.

(10) Yang, Y.; Yan, Y.; Wang, W.; Li, J. R. Precise size control of hydrophobic gold nanoparticles using cooperative effect of refluxing ripening and seeding growth. *Nanotechnology* **2008**, *19* (17), 175603–175612.

(11) Daniel, M. C.; Astruc, D. Gold nanoparticles: Assembly, supramolecular chemistry, quantum-size-related properties, and applications toward biology, catalysis, and nanotechnology. *Chem. Rev.* **2004**, *104* (1), 293–346.

(12) Esumi, K.; Suzuki, A.; Yamahira, A.; Torigoe, K. Role of poly(amidoamine) dendrimers for preparing nanoparticles of gold, platinum, and silver. *Langmuir* **2000**, *16* (6), 2604–2608.

(13) Filali, M.; Meier, M. A. R.; Schubert, U. S.; Gohy, J. F. Star-block copolymers as templates for the preparation of stable gold nanoparticles. *Langmuir* **2005**, *21* (17), 7995–8000.

(14) Shenhar, R.; Norsten, T. B.; Rotello, V. M. Polymer-mediated nanoparticle assembly: Structural control and applications. *Adv. Mater.* **2005**, *17* (6), 657–669.

(15) Sun, X. P.; Jiang, X.; Dong, S. J.; Wang, E. K. One-step synthesis and size control of dendrimer-protected gold nanoparticles: A heat-treatment-based strategy. *Macromol. Rapid Commun.* **2003**, *24* (17), 1024–1028.

(16) Taubert, A.; Wiesler, U. M.; Mullen, K. Dendrimer-controlled one-pot synthesis of gold nanoparticles with a bimodal size distribution and their self-assembly in the solid state. *J. Mater. Chem.* **2003**, *13* (5), 1090–1093.

(17) Jana, N. R. Gram-scale synthesis of soluble, near-monodisperse gold nanorods and other anisotropic nanoparticles. *Small* **2005**, *1* (8−9), 875–882.

(18) Brust, M.; Walker, M.; Bethell, D.; Schiffrin, D. J.; Whyman, R. Synthesis of thiol-derivatized gold nanoparticles in a 2-phase liquid-liquid system. *J. Chem. Soc. Chem. Commun.* **1994**, *7*, 801–802.

(19) Chen, H. J.; Kou, X. S.; Yang, Z.; Ni, W. H.; Wang, J. F. Shape- and size-dependent refractive index sensitivity of gold nanoparticles. *Langmuir* **2008**, *24* (10), 5233–5237.

(20) Han, M. Y.; Quek, C. H.; Huang, W.; Chew, C. H.; Gan, L. M. A simple and effective chemical route for the preparation of uniform nonaqueous gold colloids. *Chem. Mater.* **1999**, *11* (4), 1144–1147.

(21) Teranishi, T.; Kiyokawa, I.; Miyake, M. Synthesis of monodisperse gold nanoparticles using linear polymers as protective agents. *Adv. Mater.* **1998**, *10* (8), 596–599.

(22) Shields, S. P.; Richards, V. N.; Buhro, W. E. Nucleation control of size and dispersity in aggregative nanoparticle growth. A study of the coarsening kinetics of thiolate-capped gold nanocrystals. *Chem. Mater.* **2010**, *22*, 3212–3225.

(23) Bogush, G. H.; Zukoski, C. F. Uniform SiO_2 particle-precipitation - An aggregative growth model. *J. Colloid Interface Sci.* **1991**, *142*, 19–34.

(24) Zhu, H. T.; Zhang, C. Y.; Yin, Y. S. Rapid synthesis of copper nanoparticles by sodium hypophosphite reduction in ethylene glycol under microwave irradiation. *J. Cryst. Growth* **2004**, *270* (3−4), 722–728.

(25) Okitsu, K.; Ashokkumar, M.; Grieser, F. Sonochemical synthesis of gold nanoparticles: Effects of ultrasound frequency. *J. Phys. Chem. B* **2005**, *109* (44), 20673–20675.

(26) Sugimoto, T. Underlying mechanisms in size control of uniform nanoparticles. *J. Colloid Interface Sci.* **2007**, *309*, 106–118.

(27) Chen, S. H.; Kimura, K. Synthesis and characterization of carboxylate-modified gold nanoparticle powders dispersible in water. *Langmuir* **1999**, *15* (4), 1075–1082.

(28) Luo, Y. L. One-step preparation of gold nanoparticles with different size distribution. *Mater. Lett.* **2007**, *61* (4−5), 1039–1041.

(29) Wang, C. H.; Chien, C. C.; Yu, Y. L.; Liu, C. J.; Lee, C. H.; Chen, C. H.; Hwu, Y.; Yang, C. S.; Je, J. H.; Margaritondo, G Structural properties of 'naked' gold nanoparticles formed by synchrotron X-ray irradiation. *J. Synchrotron Radiat.* **2007**, *14*, 477–482.

(30) Wang, C. H.; Hua, T. E.; Chien, C. C.; Yu, Y. L.; Yang, T. Y.; Liu, C. J.; Leng, W. H.; Hwu, Y.; Yang, Y. C.; Kim, C. C.; Je, J. H.; Chen, C. H.; Lin, H. M.; Margaritondo, G. Aqueous gold nanosols stabilized by electrostatic protection generated by X-ray irradiation assisted radical reduction. *Mater. Chem. Phys.* **2007**, *106*, 323–329.

(31) Wang, C.-H.; Liu, C. J.; Wang, C. L.; Hua, T. E.; Obliosca, J. M.; Lee, K. H.; Hwu, Y.; Yang, C. H.; Liu, R. H.; Lin, H. M.; Je, J. H.; Margaritondo, G. Optimizing the size and surface properties of polyethylene glycol (PEG)−gold nanoparticles by intense X-ray irradiation. *J. Phys. D* **2008**, *41*, 195301.

(32) Liu, C. J.; Wang, C. H.; Wang, C. L.; Hwu, Y.; Lin, C. Y.; Margaritondo, G. Simple dose rate measurements for a very high synchrotron X-ray flux. *J. Synchrotron Radiat.* **2009**, *16*, 395–397.

(33) Gachard, E.; Remita, H.; Khatouri, J.; Keita, B.; Nadjo, L.; Belloni, J. Radiation-induced and chemical formation of gold clusters. *New J. Chem.* **1998**, *22* (11), 1257–1265.

(34) Akhavan, A.; Kalhor, H. R.; Kassaee, M. Z.; Sheikh, N.; Hassanlou, M. Radiation synthesis and characterization of protein stabilized gold nanoparticles. *Chem. Eng. J.* **2010**, *159* (1−3), 230–235.

(35) Kim, Y. G.; Oh, S. K.; Crooks, R. M. Preparation and characterization of 1−2 nm dendrimer-encapsulated gold nanoparticles having very narrow size distributions. *Chem. Mater.* **2004**, *16* (1), 167–172.

(36) Zhang, C. X.; Ren, Z. Y.; Yin, Z. G.; Qian, H. Y.; Ma, D. Z. Amide II and amide III bands in polyurethane model soft and hard segments. *Polym. Bull.* **2008**, *60* (1), 97–101.

(37) Renugopalakrishnan, V.; Kloumann, P. H. B.; Bhatnagar, R. S. L-Alanyl-glycylglycine - FT-IR and Raman-spectroscopic evidence for tripeptide packing in a collagen-like arrangement. *Biopolymers* **1984**, *23* (4), 623–627.

(38) Liu, C. J.; Wang, C. H.; Chien, C. C.; Yang, T. Y.; Chen, S. T.; Leng, W. H.; Lee, C. F.; Lee, K. H.; Hwu, Y.; Lee, Y. C.; Cheng, C. L.; Yang, C. S.; Chen, Y. J.; Je, J. H.; Margaritondo, G. Enhanced X-ray irradiation-induced cancer cell damage by gold nanoparticles treated by a new synthesis method of polyethylene glycol modification. *Nanotechnology* **2008**, *19* (29), 295104–259108.

(39) Liu, C. J.; Wang, C. H.; Chen, S. T.; Chen, H. H.; Leng, W. H.; Chien, C. C.; Wang, C. L.; Kempson, I. M.; Hwu, Y.; Lai, T. C.; Hsiao, M.; Yang, C. S.; Chen, Y. J.; Margaritondo, G. Enhancement of cell radiation sensitivity by pegylated gold nanoparticles. *Phys. Med. Biol.* **2010**, *55* (4), 931–945.

(40) Cai, X. Q.; Wang, C. L.; Chen, H. H.; Chien, C. C.; Lai, S. F.; Chen, Y. Y.; Hua, T. E.; Kempson, I. M.; Hwu, Y.; Yang, C. S.; Margaritondo, G. Tailored Au nanorods: Optimizing functionality, controlling the aspect ratio and increasing biocompatibility. *Nanotechnology* **2010**, *21* (33), 335604–335611.